APPLIED AND ENVIRONMENTAL MICROBIOLOGY, Oct. 2006, p. 6743–6750 Vol. 72, No. 10
0099-2240/06/$08.00+0 doi:10.1128/AEM.00584-06

Eukaryotic Lipid Body Proteins in Oleogenous Actinomycetes and Their Targeting to Intracellular Triacylglycerol Inclusions: Impact on Models of Lipid Body Biogenesis

Jan Hänisch,[1]† Marc Wältermann,[1]† Horst Robenek,[2] and Alexander Steinbüchel[1]*

Institut für Molekulare Mikrobiologie und Biotechnologie, Westfälische Wilhelms-Universität, Corrensstrasse 3, D-48149 Münster,[1] and Department of Cell Biology and Ultrastructural Research, Leibniz Institute for Arteriosclerosis Research, University of Münster, D-48149 Münster,[2] Germany

Received 12 March 2006/Accepted 15 July 2006

Bacterial neutral lipid inclusions are structurally related to eukaryotic lipid bodies. These lipid inclusions are composed of a matrix of triacylglycerols (TAGs) or wax esters surrounded by a monolayer of phospholipids. Whereas the monolayers of lipid bodies from animal and plant cells harbor specific classes of proteins which are involved in the structure of the inclusions and lipid homoestasis, no such proteins are known to be associated with bacterial lipid inclusions. The present study was undertaken to reveal whether the mammalian lipid body proteins perilipin A, adipose differentiation-related protein, and tail-interacting protein of 47 kDa (TIP47), which comprise the so called PAT family proteins, and the maize (*Zea mays* L.) oleosin are targeted to prokaryotic TAG bodies in vivo. When fused to enhanced green fluorescent protein, all proteins except the oleosin were mainly located at the surfaces of lipid inclusions when heterologously expressed in the recombinant actinomycetes *Rhodococcus opacus* PD630 and *Mycobacterium smegmatis* mc^{2}155. A more detailed intracellular distribution analysis of TIP47 in recombinant *R. opacus* cells by immunocytochemical labeling of ultrathin cryosections and freeze fracture replicas revealed a substantial amount of TIP47 protein also pervading the cores of the inclusions. We discuss the impact of these results on the current model of lipid body biogenesis in prokaryotes.

Most organisms are capable of accumulating hydrophobic compounds, such as triacylglycerols (TAGs), wax esters (WEs), sterol esters, or poly(hydroxyalkanoates). These lipids and polymers are deposited as intracellular inclusions and serve mainly as energy and carbon reserves or precursors for membrane lipid and steroid biosynthesis. The primary energy storage compounds in eukaryotes are TAGs, whereas most prokaryotes synthesize poly(hydroxyalkanoates) (19, 25). In bacteria, reserve TAGs and WEs are restricted mainly to nocardioform actinomycetes, streptomycetes, and some gram-negative strains (3, 32). Bacterial neutral lipid inclusions are structurally related to those in eukaryotes. Both consist of a lipid core surrounded by a monolayer of phospholipids, which shields the inclusions from the cytoplasm, thereby preventing coalescence or denaturation of cytoplasmic proteins due to hydrophobic interactions. The biogenesis and protein equipment of TAG and WE inclusions in bacteria differs significantly from eukaryotic lipid inclusions. In eukaryotes, lipid inclusions are assumed to emanate by accumulation of lipids between both phospholipid leaflets at the endoplasmic reticulum (ER) and subsequent lipid body budding. The budding particle, which has a phospholipid monolayer membrane derived from the outer ER leaflet, is finally released into the cytoplasm (5, 19). In contrast, in bacteria TAGs and WEs are synthesized by wax ester synthase/acyl-coenzyme A:diacylglycerol acyltransferase (WS/DGAT) as small enzyme-bound droplets at the cytoplasmic face of the plasma membrane. These droplets aggregate to larger structures, which are assumed to be coated by phospholipids, before they are released into the cytoplasm (12, 13, 31).

Whereas in animals and most plants the lipid body monolayer is associated with embedded proteins, no such proteins are known to surround bacterial lipid inclusions (12, 31). The perilipins are the best characterized mammalian lipid body proteins and are involved in structure and formation of the organelles and control of lipid balance, by regulating lipolysis by hormone-sensitive lipase (18). Three perilipin isoforms, A, B, and C, are encoded by alternatively spliced forms of mRNA transcribed from a single gene (9, 17). All perilipins share a common N terminus, which is also very similar to those of adipose differentiation-related protein (ADRP) and tail-interacting protein of 47 kDa (TIP47), which together with perilipin constitute the PAT protein family (16). Perilipin A is the largest isoform and the most abundant protein associated with adipocyte lipid bodies, whereas ADRP and TIP47 have a broad tissue distribution. Perilipins and ADRP are specifically associated with the lipid body surface, whereas TIP47 is also abundant in the cytoplasm (4, 18). Reports on whether PAT family proteins are synthesized on free ribosomes or are cotranslationally inserted into nascent lipid bodies along the ER, similarly to oleosins in plants, are contradictory (5, 8, 16, 21).

Oleosins are the main proteins which are associated with lipid bodies in the seeds of desiccation-tolerant plants. They are assumed to play a key role in the maintenance of stability of the lipid bodies, since they prevent them from coalescing during seed dehydration and germination (19). Oleosins are assumed to be synthesized by polyribosomes on the ER and incorporated cotranslationally into lipid bodies during the bud-

* Corresponding author. Mailing address: Institut für Molekulare Mikrobiologie und Biotechnologie, Westfälische Wilhelms-Universität, Corrensstrasse 3, D-48149 Münster, Germany. Phone: 49 (251) 833 9821. Fax: 49 (251) 833 8388. E-mail: steinbu@uni-muenster.de.

† Jan Hänisch and Marc Wältermann contributed equally to this work.

ding process. This ER-mediated targeting appears to be universal in eukaryotes, since oleosins from maize have also been successfully targeted to seed lipid bodies in *Brassica napus*, and also in recombinant yeast (*Saccharomyces cerevisiae*) (15, 27).

However, although PAT proteins and oleosins can be considered specific lipid body proteins, there are no structural homologies between the two protein classes, and an understanding of how PAT proteins and oleosins interact with the lipid body surface is still at its beginning. Here, we report on heterologous expression of eukaryotic lipid body proteins in prokaryotes accumulating TAGs and their properties of binding to bacterial TAG inclusions.

MATERIALS AND METHODS

Strains, plasmids, and culture conditions. Cells of *Escherichia coli* XL1-Blue (Stratagene) were routinely cultivated in Luria-Bertani (LB) medium (22). Cells of *Rhodococcus opacus* PD630 (DSM 44193) (2) and *Mycobacterium smegmatis* mc^{2}155 (ATCC 70084) (24) were cultivated aerobically in Standard I medium (Merck). To promote biosynthesis of TAG inclusions, cells of *R. opacus* were cultivated for 24 and 48 h in mineral salt medium (MSM) (23) with 0.1 g liter^{-1} NH_4Cl and 10 g liter^{-1} sodium gluconate as a carbon source, whereas *M. smegmatis* was cultivated under the same conditions except that 10 g liter^{-1} glucose as a carbon source was supplied (storage conditions). To maintain plasmid pJAM2 and derivatives, kanamycin was used at a final concentration of 50 μg ml^{-1} as described previously (22). Induction of the acetamidase promoter of pJAM2 and derivatives was achieved by addition of 0.5% (wt/vol) acetamide to cultures of *R. opacus* and of 0.01% acetamide to cultures of *M. smegmatis* (10, 30). The TAG content of the cells was routinely inspected by thin-layer chromatography according to a previously described method (12) and by microscopic examination. Acetamide did not alter the N limitation in cultures of *R. opacus*, since it was not metabolized, whereas it had a decreasing influence on TAG biosynthesis in *M. smegmatis*, as was described recently (10). All liquid cultures were in Erlenmeyer flasks equipped with baffles at 37°C for *E. coli* and at 30°C for *R. opacus* and *M. smegmatis*. Solid media were prepared by addition of 18 g liter^{-1} agar-agar.

Cloning of the eGFP gene downstream of the *ace* promoter of pJAM2. Standard molecular biology protocols were used (22). All PCR products were first cloned into a TA vector (pGEM-T Easy; Promega), confirmed by DNA sequencing, and then released by digestion with appropriate restriction enzymes before cloning into expression vectors (see below). To facilitate subcloning, restriction enzyme recognition sites (underlined below) were incorporated in the sequences of the oligonucleotides. A 720-bp fragment containing the complete coding sequence of the enhanced green fluorescent protein (eGFP) gene was amplified without the start codon from plasmid pEGFP-N3 (BD Bioscience Clontech) by using PCR primers egfp-5′ (5′-AAATCTAGAGTGAGCAAGGGCGAGGAG CTG-3′) and egfp-3′, harboring the native stop codon (boldface) (5′-AAATCT AGA**TTA**CTTGTACAGCTCGTCCATG-3′). The PCR product was then cloned colinear to the *ace* promoter into the XbaI site of pJAM2, an *E. coli-Mycobacteria*/*Rhodococcus* shuttle vector containing the 1.5-kbp *ace* promoter region (30), to create a 5′-terminal functional in-frame fusion with the first six codons of the *amiC* gene and yielding pJAM2-egfp.

Construction of lipid body protein-eGFP fusion-expressing plasmids. Coding regions of the respective proteins were amplified without their native start and stop codons to facilitate generation of functional 3′-terminal fusion constructs with the eGFP gene in plasmid pJAM2-egfp. The murine perilipin A-coding region (1,551 bp; NCBI accession number AAH96685) was amplified by PCR from retroviral expression vector pSRαMSVtkneo harboring murine perilipin A cDNA (8), using oligonucleotides perA-5′ (5′-AAAAGTACTTCAATGAACA AGGGCCCAACC-3′) and perA-3′ (5′-AAAAGTACTGCTCTTCTTGCGCA GCTGGC-3′). Human TIP47 cDNA (1,302 bp; NCBI accession number AAC39751) was amplified from plasmid pQE31 (7), using oligonucleotides tip47-5′ (5′-AAAGGATCCTCTGCCGACGGGGCAGAGGC-3′) and tip47-3′ (5′-AAAGGATCCTTTCTTCTCCTCCGGGGCTT-3′). Human ADRP cDNA (1,311 bp; NCBI accession number NP_001113) was amplified from an ADRP cDNA fragment provided by C. Londos (Laboratory of Cellular and Developmental Biology, National Institutes of Health, Bethesda, Md.), using oligonucleotides adrp-5′ (5′-AAAAGTACTAGTTTTATGCTCAGATCGCTGG-3′) and adrp-3′ (AAAAGTACTGCATCCGTTGCAGTTGATCCAC-3′). Each PCR product among the PAT family genes was cloned colinear to the *ace* promoter upstream of the 5′-eGFP gene region into the BamHI or ScaI site of pJAM2-egfp, creating pJAM2-perA_{mur}-egfp, pJAM2-tip47$_{hum}$-egfp and pJAM2-adrp$_{hum}$-egfp. A 567-bp fragment representing the cDNA coding region of the 18-kDa maize oleosin (NCBI accession number AAA67699) was amplified from plasmid pL2± (20) by using oligonucleotides oleo-5′ (5′-AAAGGATCCGCGG ACCGCGACCGCAGCGG-3′) and oleo-3′ (5′-AAAGGATCCCGAGGAAGC CCTGCCGCCG-3′) and was then cloned colinear to the *ace* promoter into the BamHI site of pJAM2-egfp upstream of the 5′-eGFP gene region, creating pJAM2-oleo$_{mays}$-egfp. Similarly, an eGFP fusion with a truncated maize oleosin, representing only its central hydrophobic domain (amino acids 48 to 113), was constructed by PCR using oligonucleotides oleoHD-5′ (5′-AAAGGATCCGCG CTGACGGTGGCGACGCTG-3′) and oleoHD-3′ (5′-AAAGGATCCCGCCG TGTTGGCGAGGCACGT-3′). This plasmid was referred to as pJAM2-oleoHD-egfp. Next, the eGFP portion of each fusion was released by XbaI restriction and religation from each of the expression plasmids constructed, yielding pJAM2-perA_{mur}, pJAM2-tip47$_{hum}$, pJAM2-adrp$_{hum}$, pJAM2-oleo$_{mays}$, and pJAM2-oleoHD. Since the genes in each of the constructed plasmids lacked their own stop codon but contained one after the His_6 tag linker sequence of pJAM2, the amino acids SRHHHHHH were added to the C termini of the respective proteins.

Plasmids were transferred to *R. opacus* and *M. smegmatis* by electroporation in a model 2550 electroporator (Eppendorf-Netheler-Hinz, Hamburg, Germany). Preparation of electrocompetent cells was done as described by Kalscheuer et al. (11) for *R. opacus* and by Snapper et al. (24) for *M. smegmatis*.

Preparation of crude cell extracts and soluble and lipid body fractions. Cells of *R. opacus* and *M. smegmatis* were grown in MSM with a reduced ammonium concentration as described above, harvested by centrifugation (20 min, 6,000 × *g*, 4°C), and resuspended in 2 volumes of 10 mM Tris-HCl (pH 7.5). After three passages through a French pressure cell (1,000 MPa), crude extracts were obtained. To obtain soluble fractions, cell debris was eliminated from crude extracts by centrifugation for 30 min at 16,000 × *g* at 4°C, and the clear supernatant was used for further experiments. Lipid bodies were prepared by loading 1 to 2 ml of crude extracts on the top of a discontinuous glycerol gradient. The discontinuous glycerol gradient consisted of 3 ml each of 22, 44, and 88% (vol/vol) glycerol in 10 mM Tris-HCl (pH 7.5). The gradient was centrifuged for 1 h at 170,000 × *g* at 4°C. The TAG inclusions were withdrawn, washed twice in 10 mM Tris-HCl (pH 7.5), and used for further analyses.

Immunoblot analysis. Known amounts of cell lysates or subcellular fractions based on equivalent protein concentrations were resolved in sodium dodecyl sulfate (SDS)-polyacrylamide gels and transferred onto a polyvinylidene membrane according to the method of Towbin et al. (29). Proteins on the membrane were stained with Ponceau S and analyzed immunologically with polyclonal chicken anti-maize oleosin immunoglobulin Gs (IgGs) (20), polyclonal rabbit anti-murine PAT IgGs (a gift from C. Londos), a polyclonal antibody raised in guinea pig against a synthetic polypeptide representing the N terminus (amino acids 1 to 16) of human TIP47 (GP30; Progen Biotechnik), and a mouse monoclonal antibody to a synthetic peptide representing the N terminus (amino acids 5 to 27) of human ADRP (AP125; Progen Biotechnik). IgGs were visualized on immunoblots by using goat anti-rabbit, anti-murine, or anti-chicken IgG–alkaline phosphatase conjugates, converting 5-bromo-4-chloro-3-indolyl-phosphate dipotassium/nitrotetrazolium blue chloride into an insoluble, dark product (Sigma).

Microscopy. Cells of *R. opacus* and *M. smegmatis* and isolated lipid inclusions were resuspended in 10 mM Tris-HCl, pH 7.5. Cells and lipid inclusions were attached to glass slides through electrostatic interaction, made positively charged through adsorption of poly-L-lysine hydrobromide. In order to coat a glass surface with poly-L-lysine hydrobromide, cleaned glass slides were rinsed thoroughly with tap water, dipped in methanol, and again rinsed with demineralized water, after which a drop of 0.01% (wt/vol) poly-L-lysine hydrobromide solution was added. After air drying, the slide was rinsed with demineralized water, and a drop of the bacterial cell or lipid inclusion suspension was added. After 15 min, the coated slide was rinsed with demineralized water to remove loosely attached cells and lipid inclusions and transferred for fluorescence microscopy. Slides were examined by conventional microscopy in a Leitz Laborlux K microscope with a 100× phase-contrast oil immersion objective. Fluorescence labeling of intracellular lipids and isolated lipid inclusions was performed by incubating samples in 0.5 μg ml^{-1} Nile Red in 10 mM (stock solution, 0.5 mg ml^{-1} in dimethyl sulfoxide). eGFP and Nile Red fluorescences were excited using a 1-λPloemak incident illuminator equipped with a 50-W mercury lamp and Leitz N2, L2, and A2 filter blocks. Recording of images was performed using a Kappa DX20 L charge-coupled device camera connected with a standard PC.

Freeze fracturing, cryosectioning, and immunogold labeling. For cryosectioning, cell suspensions were prefixed for 5 min by adding an equal volume of 4% (wt/vol) paraformaldehyde in phosphate-buffered saline (pH 7.4). Cells were

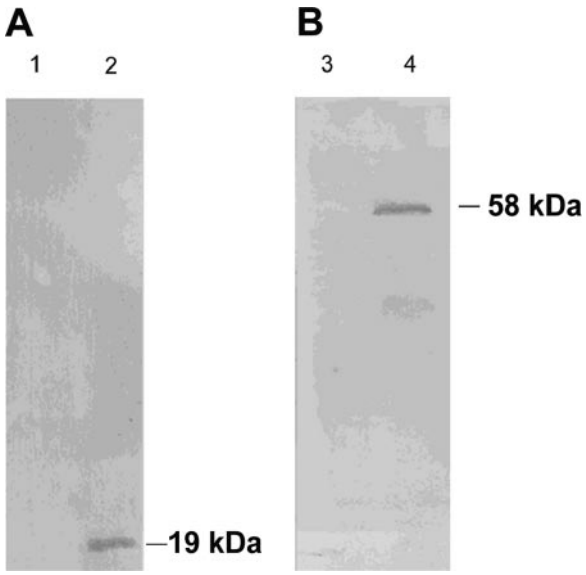

FIG. 1. Immunological detection of maize oleosin (A) and murine perilipin A (B) expression in crude protein extracts of recombinant cells of *M. smegmatis*. Cells were grown in MSM for 48 h in the presence of 0.01% (wt/vol) acetamide. Whole-cell proteins were prepared from *M. smegmatis* cells, separated by SDS-gel electrophoresis, blotted on polyvinylidene difluoride membranes, and probed with chicken anti-oleosin IgGs (A) and rabbit anti-murine PAT IgGs (B). Lanes 1 and 3, *M. smegmatis* pJAM2; lane, 2 *M. smegmatis* pJAM2-oleo$_{mays}$; lane 4, *M. smegmatis* pJAM2-perA$_{mur}$.

washed briefly in the same buffer and fixed further in 4% (wt/vol) paraformaldehyde for 1 h, followed by incubation in 4% (wt/vol) paraformaldehyde with 0.9 M sucrose and 90% (wt/vol) polyvinylpyrrolidone 25 buffered with 50 mM sodium carbonate (pH 7.0) as a cryoprotectant for 1 h. The cells were concentrated by centrifugation, placed on pins in a small volume of cryoprotectant, and frozen in liquid nitrogen. Ultrathin sectioning was performed as described by Tokuyasu (28). For freeze fracturing, cell suspensions (700 ml) were pelleted by centrifugation for 30 min at 6,000 × *g* and 4°C, resuspended in 30% (vol/vol) glycerol (<30 s), fixed in Freon 22 cooled with liquid nitrogen, and freeze fractured in a BA310 freeze fracture unit (Balzer AG) at −100°C. Replicas of the freshly fractured cells were immediately made by electron beam evaporation of platinum-carbon at angles of 38° and 90° and to thicknesses of 2 and 20 nm. The replicas were incubated overnight in 5% (wt/vol) SDS to remove cellular material except for those molecules adhering directly to the replicas, washed in distilled water, and incubated briefly in 5% (wt/vol) bovine serum albumin before immunostaining. For immunostaining of freeze fracture replicas and cryosections, the same primary antibodies as mentioned above were used, followed by donkey anti-guinea pig–18-nm-gold conjugate, goat anti-murine–12-nm-gold conjugate, or goat anti-rabbit–12-nm-gold conjugate (all from Jackson Immunoresearch), respectively. A primary antibody against eGFP was raised in rabbit (BD Biosciences) to reveal the cellular distribution of eGFP fusions by means of their eGFP tag. Control specimens, prepared without the first antibody, were essentially free of gold particles.

RESULTS

Expression of eukaryotic lipid body proteins in recombinant actinomycetes. The coding regions of the murine perilipin A, human ADRP, human TIP47, and maize oleosin genes were cloned as His$_6$-tagged fusions into the *E. coli-Rhodococcus/Mycobacterium* shuttle vector pJAM2. Crude extracts of the respective transformed *M. smegmatis* and *R. opacus* cells were analyzed for their perilipin A, ADRP, TIP47, and oleosin expression by SDS-polyacrylamide gel electrophoresis and immunoblotting, using the antibodies listed in Materials and Methods. None of the antibodies recognized any protein in untransformed *Rhodococcus/Mycobacterium* cells. The chicken anti-maize oleosin IgG easily recognized a 19-kDa protein in *M. smegmatis* cells transformed with pJAM2-oleo$_{mays}$ (Fig. 1). However, in cells of *R. opacus* harboring pJAM2-oleo$_{mays}$, expression was significantly lower and was observable only on overexposed immunoblots, even if compared to *M. smegmatis* cells not induced with acetamide (not shown). This 19-kDa protein should be the His$_6$-tagged oleosin derived from the maize gene in pJAM2-oleo$_{maize}$. No proteolytic degradation products of lower molecular mass were detected in *R. opacus* and *M. smegmatis*, indicating that the protein was stable against intracellular proteolysis. Expression of the His$_6$-tagged murine perilipin A in *M. smegmatis* and *R. opacus* harboring plasmid pJAM2-*perA*$_{mur}$ resulted in a single signal of 58 kDa on immunoblots for both strains, with intensities similar to that of recombinant oleosin expression, indicating that the protein was also stable and that intracellular proteolysis did not occur (see Fig. 1 for *M. smegmatis*). In crude extracts of *M. smegmatis* and *R. opacus* harboring pJAM2-tip47$_{hum}$ or pJAM2-adrp$_{hum}$, respectively, no observable synthesized protein could be detected on immunoblots (Table 1). Thin-layer chromatography of total lipid extracts and fluorescence microscopy using Nile Red as a dye revealed that the presence of the plasmids and expression of the proteins in *R. opacus* did not alter the lipid content of the cells or the number, shape, or size of the lipid inclusions compared to those of the wild type in presence or absence of acetamide. In contrast to this, wild-type and recombinant cells of *M. smegmatis* contained significantly decreased amounts of TAGs and numbers of lipid inclusions when more than 0.01% (wt/vol) acetamide was added to the cultures (Table 2).

TABLE 1. Synthesis of proteins in recombinant strains harboring lipid body protein expression plasmids

Plasmid	Concn of acetamide (%, wt/vol)	Protein synthesis in strain:	
		M. smegmatis mc^{2}155	*R. opacus* PD630
pJAM2-egfp	0	Low	Low
	0.01	High	
	0.5		Low
pJAM2-perA$_{mur}$	0	Low	Low
	0.01	High	
	0.5		Low
pJAM2-adrp$_{hum}$	0	Low	Low
	0.01	Low	
	0.5		Low
pJAM2-tip47$_{hum}$	0	Low	Low
	0.01	Low	
	0.5		Low
pJAM2-oleo$_{mays}$	0	Low	Low
	0.01	High	
	0.5		Low

Fluorescence localization of PAT protein and oleosin fusions in recombinant actinomycetes. We performed experiments to localize perilipin A and maize oleosin in subcellular fractions of recombinant *R. opacus* by immunoblot analysis,

TABLE 2. Accumulation of TAGs during 48 h of growth in MSM in the presence of different concentrations of acetamide as revealed by thin-layer chromatography

Concn of acetamide (%, wt/vol)	TAG accumulation in strain:	
	M. smegmatis mc^{2}155	*R. opacus* PD630
0	High	High
0.1	Low	High
0.5	Very low	High

but these failed due to the small amounts of protein that were synthesized and the low sensitivity of the immunoblot assay. The lipid body proteins were visualized in recombinant strains as fusions with eGFP to reveal the subcellular localization and binding of PAT proteins and oleosin to bacterial TAG inclusions. Cells of *R. opacus* and *M. smegmatis* were transformed with the respective PAT protein-eGFP fusion expression plasmids. Subsequently, cells were cultivated for 0, 24, and 48 h under storage conditions and inspected for their fluorescence pattern. Cells harboring plasmid pJAM2-egfp expressing unfused eGFP served as a negative control. Under these conditions and during these periods of time, cells increased their lipid content and accumulated large amounts of lipid inclusions in the cytoplasm, which were derived from peripheral lipid domains according to earlier observations (6, 31). Unfused eGFP showed a broad and diffuse fluorescence throughout the cytoplasm in *R. opacus* and *M. smegmatis*. The fluorescence was excluded from large lipid inclusions occurring in later stages of lipid accumulation (Fig. 2A). However, images obtained from *M. smegmatis* were poor compared to those obtained from *R. opacus* due to its distinct confluent growth and smaller cell size, but they corresponded well to all the results obtained for recombinant strains of *R. opacus*. In contrast, strains harboring pJAM2-perA_{mur}-egfp exhibited fluorescence exclusively in small lipid inclusions attached to the plasma membrane in early stages of lipid accumulation. During proceeding TAG accumulation and formation of cytoplasmic lipid inclusions, perilipin A-eGFP fluorescence appeared to be associated with cytoplasmic lipid inclusions, often observed as peripheral rings surrounding the inclusions (Fig. 2B). The lipid inclusions were isolated from the respective recombinant *R. opacus* strains and investigated by fluorescence microscopy to determine if this fluorescence pattern was not resulting from simple exclusion of perilipin A-eGFP fluorescence from the lipid inclusions. In addition, the lipids in the cores of the inclusions were stained with Nile Red. Isolated inclusions from cells expressing perilipin A-eGFP exhibited a clear ring-shaped fluorescence at their surface, with red fluorescence of the lipid core caused by the incorporated Nile Red dye (Fig. 2C). In contrast, lipid inclusions in cells expressing unfused eGFP exhibited no fluorescence when observed without Nile Red labeling. These data indicate that perilipin A-eGFP associates closely with the surface of lipid inclusions in recombinant *R. opacus* and also remains stably associated during the cell disruption process.

Time-lapse experiments testing the subcellular localization of ADRP-eGFP and TIP47-eGFP in recombinant *R. opacus* strains harboring pJAM2-adrp_{hum}-egfp or pJAM2-tip47$_{hum}$-egfp, respectively, were also performed. Both recombinant strains synthesized lipid inclusions similar to those observed in the wild type and the strain expressing perilipin A-eGFP. In contrast to our immunoblot analysis, clear fluorescence was observable in *R. opacus* harboring pJAM2-tip47$_{hum}$-egfp. The fluorescence was localized exclusively to intracellular, peripheral lipid domains at the beginning of lipid accumulation. After

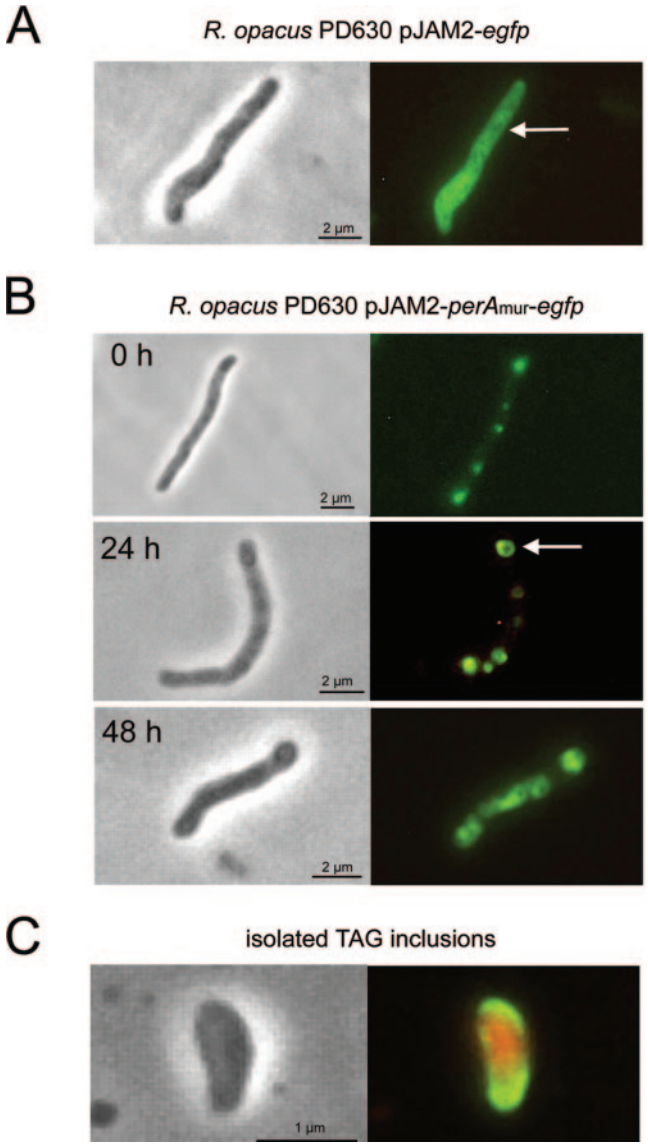

FIG. 2. Distribution of eGFP fusion of perilipin A in recombinant *R. opacus*. The left panels shows phase-contrast images, whereas the right panels shows the corresponding fluorescence images. (A) A pJAM2-egfp-transformed cell of *R. opacus* grown for 24 h under storage conditions shows a diffuse cytoplasmic fluorescence of unfused eGFP. The arrow indicates an area excluded from fluorescence due to an intracellular, unmarked TAG inclusion. (B) Cells transformed with pJAM2-perA_{mur}-egfp grown for 0, 24, or 48 h under storage conditions, expressing eGFP-fused murine perilipin A. Fluorescence of the eGFP fusion is associated with intracellular TAG inclusions (arrow). (C) TAG inclusion isolated from a perilipin A-eGFP-expressing *R. opacus* cell grown for 48 h under storage conditions. After isolation of the TAG inclusion, counterstaining of core lipids was performed with Nile Red.

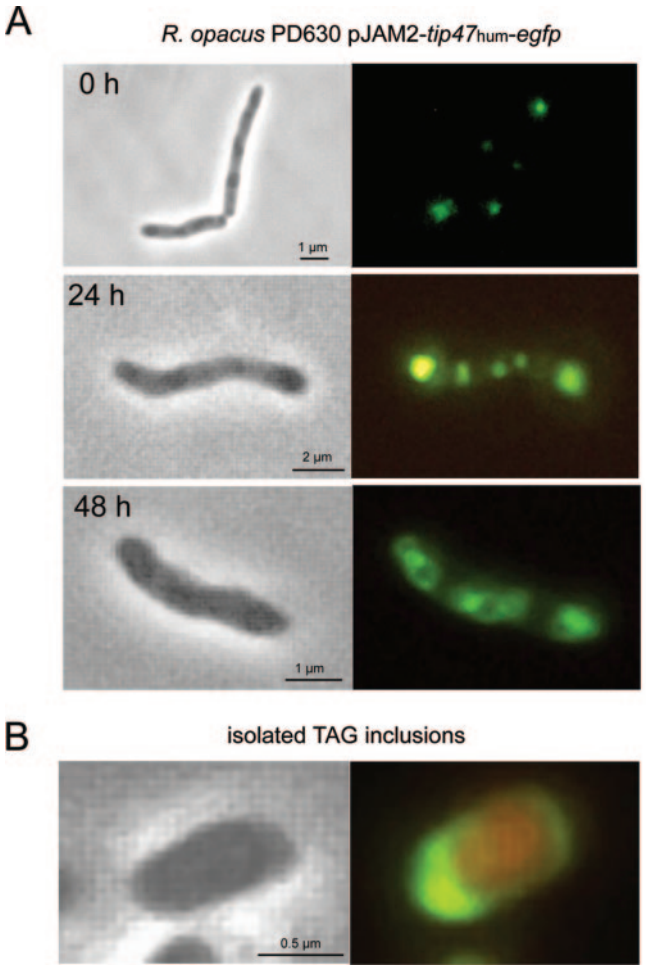

FIG. 3. Distribution of eGFP fusion of TIP47 in recombinant *R. opacus*. Phase-contrast images are depicted in the left panels and corresponding fluorescence images in the right panels. (A) Time-lapse experiment demonstrating the formation of intracellular TAG inclusions and association of TIP47-eGFP protein with these inclusions in recombinant *R. opacus*. (B) Isolated TAG inclusion contrasted with Nile Red carrying associated TIP47-eGFP fusions. TAG inclusions were isolated from cultured cells grown for 48 h under lipid storage conditions.

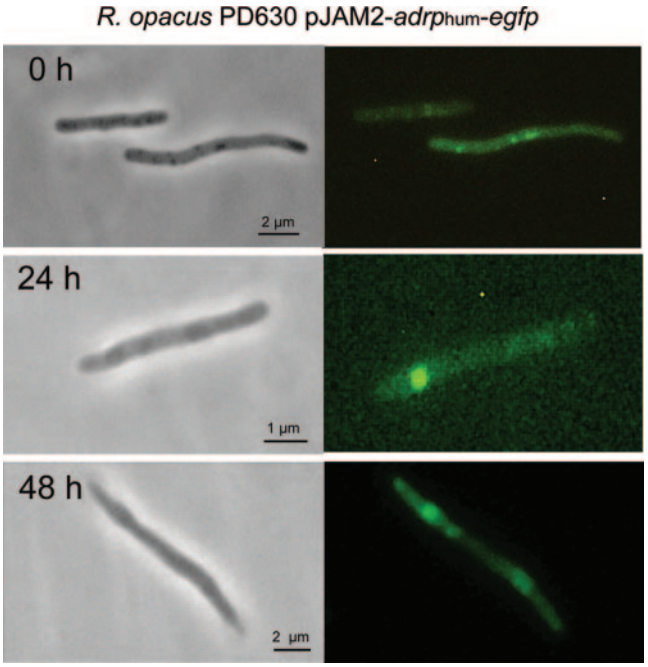

FIG. 4. Distribution of eGFP fusion of ADRP in recombinant *R. opacus*. Phase-contrast images (left panels) and corresponding fluorescence images (right panels) are shown. Cells were transformed with pJAM2-adrp$_{hum}$-egfp and grown for 0, 24, and 48 h under storage conditions.

24 and 48 h under storage conditions, large cytoplasmic lipid inclusions occurred. Similarly to the results obtained for *R. opacus* synthesizing perilipin A-eGFP, TIP47-eGFP fluorescence was often observed in the form of rings surrounding large lipid inclusions (Fig. 3A). This labeling pattern was also confirmed on isolated inclusions tagged with TIP47-eGFP (Fig. 3B). In the strain harboring pJAM2-adrp$_{hum}$-egfp, fluorescence was very weak in early stages of lipid accumulation but was clearly distinguishable from autofluorescence in control experiments performed with wild-type *R. opacus*. ADRP-eGFP was clearly visible in lipid inclusions after 24 and 48 h of lipid accumulation. However, background fluorescence was also observed, which might be due to the prolonged exposure time during image recording (Fig. 4).

Fluorescence was also obtained in *M. smegmatis* and *R. opacus* harboring pJAM2-oleo$_{mays}$-egfp; however, in contrast to the observations with PAT family proteins, fluorescence was similar to that of the control strains expressing unfused eGFP, indicating that the distribution of the oleosin fusion does not correlate with any of the intracellular structures (not shown). Additional experiments were performed with an eGFP fusion to a truncated oleosin, which possessed only its hydrophobic domain. However, besides a significantly lower fluorescence in the respective recombinant cells, results were very similar to those for the native protein and exhibited no preferential location of fluorescence. Lipid inclusions from strains expressing the native and truncated oleosin exhibited no fluorescence when purified from cell lysatesm (Table 3).

Immunogold labeling of cryosections and freeze fracture replicas of recombinant *R. opacus*. We performed postembedding immunogold labeling on cryosections by using antibodies raised against the PAT family proteins and the eGFP tag listed in Materials and Methods to verify the exclusive localization of PAT family proteins on intracellular TAG inclusions in *R. opacus* and *M. smegmatis* as revealed by the fluorescence microscopic investigations. However, immunogold-labeled cryosections of recombinant cells of *R. opacus* and *M. smegmatis* expressing eGFP fusions of perilipin A or ADRP were indistinguishable from those in the respective control experiments, which, in the case of ADRP, might be due to the small amount of protein synthesized. Only experiments using the guinea pig anti-human TIP47 antibodies yielded reliable results, and corresponding to our preceding observations, TIP47-eGFP was associated exclusively with the TAG inclusions in *R. opacus* harboring pJAM2-tip47$_{humr}$-egfp (Fig. 5A).

Since formation of TAG inclusions in bacteria is an emulsion aggregation-driven process, which could cause an encap-

TABLE 3. Fluorescence localization of eGFP-tagged lipid body proteins in recombinant actinomycetes[a]

Plasmid	*M. smegmatis* mc²155		*R. opacus* PD630	
	Fluorescence intensity	Localization	Fluorescence intensity	Localization
pJAM-egfp	Strong	Diffuse	Strong	Diffuse
pJAM-perA$_{mur}$-egfp	Strong	TAG inclusion associated	Strong	TAG inclusion associated
pJAM-adrp$_{hum}$-egfp	Low	TAG inclusion associated	Low	TAG inclusion associated
pJAM-tip47$_{hum}$-egfp	Strong	TAG inclusion associated	Strong	TAG inclusion associated
pJAM-oleo$_{mays}$-egfp	Low	Diffuse	Low	Diffuse
pJAM-oleoHD-egfp	Very low	Diffuse	Very low	Diffuse

[a] The following are general characteristics relevant for fluorescence microscopic localization of eGFP-tagged lipid body proteins: for *M. smegmatis* mc²155, confluent growth, small cell size (0.8 by 3 μm), and small TAG inclusions (200 to 300 nm in diameter); for *R. opacus* PD630, single cells, large cell size (1.2 by 5 μm), and large TAG inclusions (200 to 500 nm in diameter).

sulation of lipid-binding proteins into the lipid core, freeze fracture experiments were carried out to reveal the distribution of PAT family proteins on the surfaces and cores of TAG inclusions in the recombinant cells. In general, when bacterial cells are freeze fractured, the fracture plane runs between both leaflets of cellular membranes. Sometimes the fracture plane runs across the cells and intracellular lipid inclusions, enabling a cross-fractured view into the cores of the inclusions. In freeze fracture replicas of *R. opacus*, a series of tightly compressed, alternately oriented lipid layers of various depths appeared throughout the fractured cores of TAG inclusions, similar to those previously observed in cross-fractured eukaryotic and prokaryotic TAG inclusions (21, 31). The outermost of these layers is thought to originate from the surrounding phospholipid layer. For immunogold labeling of PAT proteins in freeze fracture replicas, recombinant cells of *R. opacus* were grown under storage conditions for 48 h. Corresponding to the labeling experiments on cryosections, labeled replicas of ADRP- and perilipin A-expressing cells of *R. opacus* showed no reliable results and were indistinguishable from the respective controls. However, after labeling of the replicas obtained from the strain harboring pJAM2-tip47$_{hum}$, a variety of locations within the lipid inclusions were labeled (Fig. 5B and C). No significant labeling of the surroundings of the cells, the cytoplasm, and the different faces of the plasma membrane was obtained. The distribution of TIP47 in recombinant *R. opacus* was also confirmed on replicas of the respective strain expressing the eGFP-tagged TIP47, in which labeling was performed using rabbit anti-eGFP IgG as the primary antibody (Fig. 5C).

DISCUSSION

In this study we demonstrated the synthesis of the mammalian lipid body proteins perilipin A, ADRP, and TIP47 in two different actinomycetes accumulating TAGs and their targeting to intracellular TAG inclusions (Tables 1, 2, and 3). Perilipins and ADRP were previously exclusively found associated with lipid bodies in eukaryotic cells, but the mechanisms by which they are targeted to the lipid bodies remained unclear (5). In bacteria, the PAT family proteins, which are most probably synthesized at free ribosomes in the cytoplasm, must interact directly with the lipid inclusion surface, because an indirect anchorage mediated by other specific proteins can be excluded because they should be absent in the prokaryotic systems. Sequences for targeting of a few lipid droplet proteins have been reported in the literature. For example, the targeting and anchorage of perilipins are assumed to be mediated by three hydrophobic sequences in the central 25% region of the protein, although the exact targeting mechanism remains to be elucidated (26). Freeze fracture immunogold labeling showed that TIP47 was present not only on the amphipathic surface but also in the hydrophobic core of the TAG inclusions in recombinant *R. opacus*. Since PAT proteins do not represent outstanding hydrophobic proteins, it is unlikely that a diffusion of the proteins into the core of the inclusions across the phospholipid monolayer occurs. This distribution pattern must be due to the special mechanism by which lipid inclusions in bacteria are formed. In bacteria, TAGs are synthesized as small WS/DGAT-associated droplets at the cytoplasmic face of the plasma membrane. The association of WS/DGAT molecules with nascent lipid droplets forms an oleogenous, emulsive layer. These small, enzyme-bound lipid droplets aggregate/coalesce to lipid prebodies and are then released from the membrane to form cytoplasmically localized lipid inclusions during proceeding lipid synthesis (31). By association of the PAT proteins with the surfaces of these small lipid droplets bound in the oleogenous layer and subsequent coalescence of the droplets, an encapsulation of PAT proteins into the hydrophobic core of lipid inclusions could occur.

In contrast to the PAT proteins, the native and truncated maize oleosin failed to bind to the TAG inclusions in recombinant *R. opacus* and *M. smegmatis*. An outstanding feature of oleosins is their central hydrophobic domain consisting of long antiparallel β-structures (14). The central domain penetrates directly into the lipid core, whereas the N- and C-terminal regions locate at the surface of the lipid body, thereby forming a meshwork-like organization. A proline knot motif located at the central loop of its hydrophobic domain was recognized as a putative targeting signal (1). In plants oleosins are synthesized and incorporated into nascent lipid bodies along the ER, allowing the oleosins to enter the lipid body without exposing their hydrophobic domain to the cytoplasm. The results of this study provided further evidence that this mechanism seems to be essential for the targeting of oleosins, since bacteria do not possess an ER. However, although only one oleosin has been tested so far for its targeting behavior in TAG-accumulating bacteria, our findings are in contrast to the "postencasement" model for the biogenesis of plant lipid bodies, in which oleosins translocate to preexisting lipid bodies which could arise naked from the ER (33).

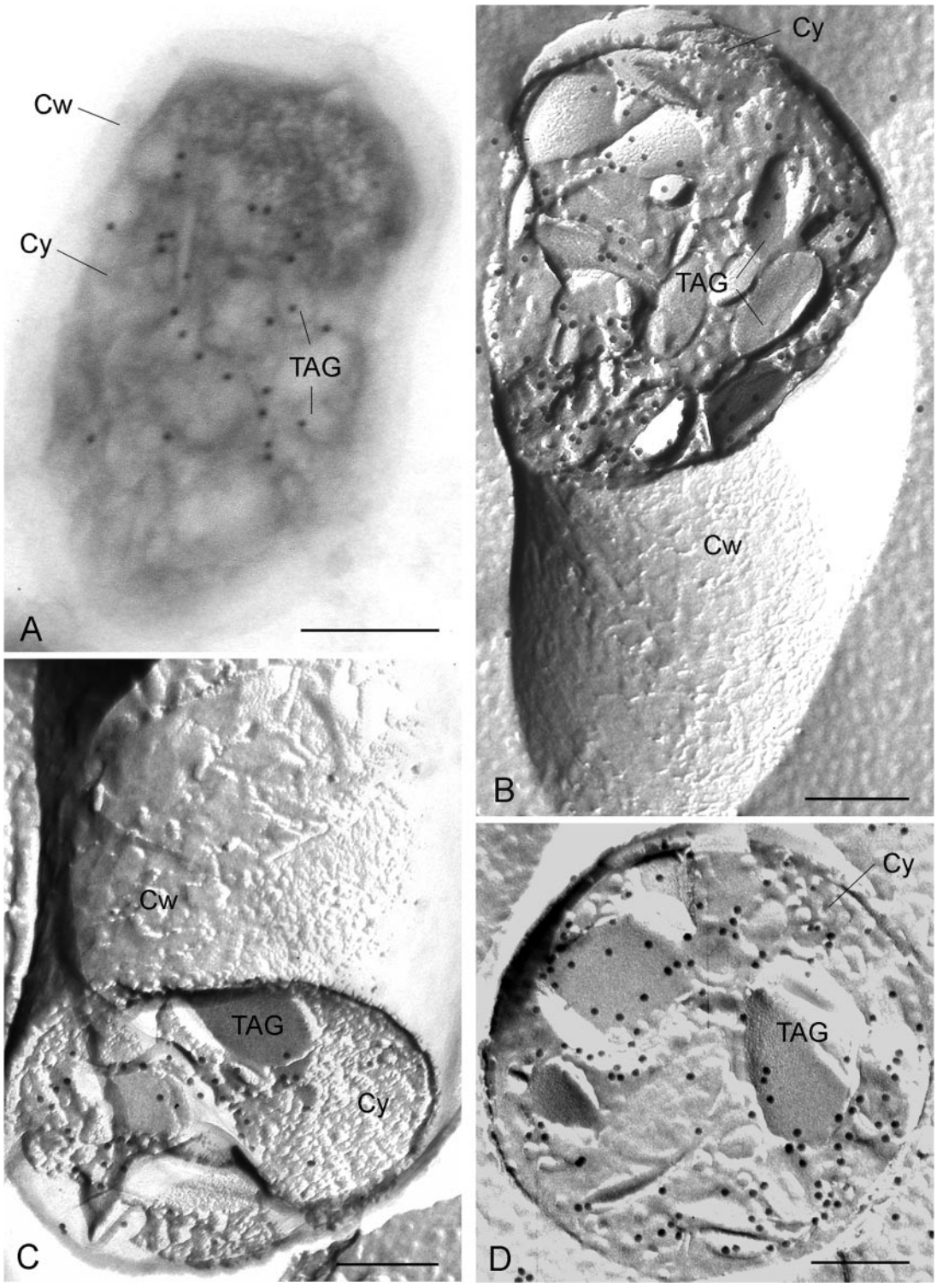

FIG. 5. Immunogold labeling of TIP47 in cytoplasmic TAG inclusions of cryosectioned and freeze fractured recombinant *R. opacus* cells. (A) Immunogold labeling of TIP47 on a cryosection with guinea pig anti-human IgGs followed by 18-nm-gold-conjugated donkey anti-guinea pig IgGs. Cells were transformed with pJAM2-tip47 and grown for 24 h under storage conditions. (B and C) Immunogold (12-nm gold) labeling of the fusion protein of its TIP47 portion over the cores of intracellular TAG inclusions in concavely (B) and convexly (C) fractured cells. (D) Immunogold (12-nm gold) labeling of TIP47-eGFP by means of the eGFP tag in the cores of cross-fractured TAG inclusions in cells of *R. opacus* harboring pJAM2-tip47-egfp. Cw, cell wall; Cy, cytoplasm; TAG, TAG inclusions. Bars, 200 nm.

Our experiments demonstrate that studies on the formation of bacterial lipid inclusions and targeting of eukaryotic lipid body proteins to these lipid inclusions are a suitable tool to reveal their underlying mechanisms. In addition, PAT family proteins could be used as linkers to anchor biotechnologically relevant enzymes on the surface of bacterial lipid inclusions, which could be tailored for a variety of biotechnological applications.

ACKNOWLEDGMENTS

We are grateful for financial support from the Deutsche Forschungsgemeinschaft (STE 386/7-2 and STE 386/7-3).

We thank C. Londos (National Institutes of Health, Bethesda, Md.) for providing the ADRP cDNA and anti-PAT antibodies. We are also indebted to Dawn L. Brasaemle (Department for Nutritional Sciences, University of Wisconsin, Madison) for providing plasmids pSRαMSVtkneo and pQE31 and to A. H. C. Huang (Center for Plant Cell Biology, University of California—Riverside) for providing plasmid pL2± and anti-oleosin IgGs. We thank Karin Schlattmann and Christina Köppler for competent and indispensable technical assistance.

REFERENCES

1. **Abell, B. M., L. A. Holbrook, M. Abenes, D. J. Murphy, M. J. Hills, and M. M. Moloney.** 1997. Role of the proline knot motif in oleosin endoplasmic reticulum topology and oil body targeting. Plant Cell **9:**1481–1493.
2. **Alvarez, H. M., F. Mayer, D. Fabritius, and A. Steinbüchel.** 1996. Formation of intracytoplasmic lipid inclusions by *Rhodococcus opacus* PD630. Arch. Microbiol. **165:**377–386.
3. **Alvarez, H. M., and A. Steinbüchel.** 2002. Triacylglycerols in prokaryotic microorganisms. Appl. Microbiol. Biotechnol. **60:**367–376.
4. **Barbero, P., E. Buell, S. Zulley, and S. R. Pfeffer.** 2001. TIP47 is not a component of lipid droplets. J. Biol. Chem. **276:**24348–24351.
5. **Brown, D. A.** 2001. Lipid droplets. Proteins floating on a pool of fat. Curr. Biol. **11:**446–449.
6. **Christensen, H., N. J. Garton, R. W. Horobin, D. E. Minnikin, and M. R. Barer.** 1999. Lipid domains of mycobacteria studied with fluorescent molecular probes. Mol. Microbiol. **31:**1561–1572.
7. **Diaz, E., and S. R. Pfeffer.** 1998. TIP47: a cargo selection device for mannose 6-phosphate receptor trafficing. Cell **93:**433–443.
8. **Garcia, A., A. Sekowski, V. Subramanian, and D. L. Brasaemle.** 2003. The central domain is required to target and anchor perilipin A to lipid droplets. J. Biol. Chem. **278:**625–635.
9. **Greenberg, A. S., J. J. Egan, S. Wek, M. C. Moos, C. Londos, and A. R. Kimmel.** 1993. Isolation of cDNAs of perilipin A and perlipin B—sequence and expression of lipid-droplet associated proteins of adipocytes. Proc. Natl. Acad. Sci. USA **90:**12035–12039.
10. **Hänisch, J., M. Wältermann, H. Robenek, and A. Steinbüchel.** The *Ralstonia eutropha* H16 phasin PhaP1 targets to intracellular triacylglycerol inclusions in *Rhodococcus opacus* PD630 and *Mycobacterium smegmatis* mc^{2}155 and provides an anchor to target other proteins. Microbiology, in press.
11. **Kalscheuer, R., M. Arenskötter, and A. Steinbüchel.** 1999. Establishment of a gene transfer system for *Rhodococcus opacus* PD630 based on electroporation and its application for recombinant biosynthesis of poly(3-hydroxyalkanoic acids). Appl. Microbiol. Biotechnol. **52:**508–515.
12. **Kalscheuer, R., and A. Steinbüchel.** 2003. A novel bifunctional wax ester synthase/acyl-CoA:diacylglycerol acyltransferase mediates wax ester and triacylglycerol biosynthesis in *Acinetobacter calcoaceticus* ADP1. J. Biol. Chem. **287:**8075–8082.
13. **Kalscheuer, R., T. Stöveken, H. Luftmann, U. Malkus, R. Reichelt, and A. Steinbüchel.** 2005. Neutral lipid biosynthesis in engineered *Escherichia coli*: Jojoba like wax esters and fatty acid butyl esters. Appl. Environ. Microbiol. **72:**1373–1379.
14. **Lacey, D. J., J. Wellner, F. Beaudoin, J. A. Napier, and P. R. Shewry.** 1998. Secondary structure of oleosins in oil bodies isolated from seeds of safflower (*Carthamus tinctorius* L.) and sunflower (*Helianthus annuus* L.). Biochem. J. **334:**469–477.
15. **Lee, W. S., J. T. C. Tzen, J. C. Kridl, S. E. Radke, and A. H. C. Huang.** 1991. Maize oleosin is correctly targeted to seed oil bodies in *Brassica napus* transformed with the maize oleosin gene. Proc. Natl. Acad. Sci. USA **88:**6181–6185.
16. **Londos, C., D. L. Brasaemle, C. J. Schultz, J. P. Segrest, and A. R. Kimmel.** 1999. Perilipins, ADRP, and other proteins that associate with intracellular neutral lipid droplets in animal cells. Semin. Cell Dev. Biol. **10:**51–58.
17. **Lu, X., J. Grucia-Gray, N. G. Copeland, D. J. Gilbert, N. A. Jenkins, C. Londos, and A. R. Kimmel.** 2001. The murine perilipin gene: the lipid-droplet-associated perilipins derive from tissue-specific, mRNA splice variants and define a gene family of ancient origin. Mamm. Genome **12:**741–749.
18. **Miura, S., J. W. Gan, J. Brzostowski, M. J. Parisi, C. J. Schultz, C. Londos, B. Oliver, and A. R. Kimmel.** 2002. Functional conservation for lipid storage droplet association amoung perilipin, ADRP, and TIP47 (PAT)-related proteins in mammals, *Drosophila* and *Dictyostelium*. J. Biol. Chem. **277:**32253–32257.
19. **Murphy, D. J.** 2001. The biogenesis and function of lipid bodies in animals, plants and microorganisms. Prog. Lipid Res. **40:**325–438.
20. **Qu, R. D., and A. H. C. Huang.** 1990. Oleosin KD18 on the surface of oil bodies in maize. Genomic and cDNA sequences and the deduced protein structure. J. Biol. Chem. **265:**2238–2243.
21. **Robenek, H., M. J. Robenek, and D. Troyer.** 2005. PAT family proteins pervade lipid droplet cores. J. Lipid Res. **46:**1331–1338.
22. **Sambrook, J., E. F. Fritsch, and T. Maniatis.** 1989. Molecular cloning: a laboratory manual, 2nd ed., p. A1. Cold Spring Harbor Laboratory, Cold Spring Harbor, N.Y.
23. **Schlegel, H. G., H. Kaltwasser, and G. Gottschalk.** 1961. Ein Submersverfahren zur Kultur wasserstoffoxidierender Bakterien: Wachstumsphysiologische Untersuchungen. Arch. Mikrobiol. **38:**209–222.
24. **Snapper, S. B., R. E. Melton, S. Mustafa, T. Kieser, and W. R. Jacobs.** 1990. Isolation and characterization of efficient plasmid transformation mutants of *Mycobacterium smegmatis*. Mol. Microbiol. **4:**1911–1919.
25. **Steinbüchel, A.** 1996. PHB and other polyhydroxyalkanoic acids, p. 403–464. *In* H. J. Rehm, G. Reed, A. Pühler, and P. Stadler (ed.), Biotechnology, 2nd ed., vol. 6. Wiley VCH, Heidelberg, Germany.
26. **Subramanian, V., A. Garcia, A. Sekowski, and D. L. Brasaemle.** 2004. Hydrophobic sequences target and anchor perilipin A to lipid droplets. J. Lipid Res. **45:**1983–1991.
27. **Ting, J. T. L., R. A. Balsamo, C. Ratnayake, and A. H. C. Huang.** 1997. Oleosin of plant seed oil body is correctly targeted to the lipid bodies in transformed yeast. J. Biol. Chem. **272:**3699–3705.
28. **Tokuyasu, K. T.** 1980. Immunocytochemistry on ultrathin frozen sections. Histochem. J. **12:**381–403.
29. **Towbin, H., T. Staehelin, and J. Gordon.** 1979. Electrophoretic transfer of proteins from polyacrylamide gels to nitrocellulose sheets: procedure and some applications. Proc. Natl. Acad. Sci. USA **76:**4350–4354.
30. **Triccas, J. A., T. Parish, W. J. Britton, and B. Gicquel.** 1998. An inducible expression system permitting the efficient purification of a recombinant antigen from *Mycobacterium smegmatis*. FEMS Microbiol. Lett. **167:**151–156.
31. **Wältermann, M., A. Hinz, H. Robenek, D. Troyer, R. Reichelt, U. Malkus, H. J. Galla, R. Kalscheuer, T. Stöveken, P. von Landenberg, and A. Steinbüchel.** 2005. Mechanism of lipid-body formation in prokaryotes: how bacteria fatten up. Mol. Microbiol. **55:**750–763.
32. **Wältermann, M., and A. Steinbüchel.** 2005. Neutral lipid bodies in prokaryotes: recent insights into structure, formation, and relationship to eukaryotic lipid depots. J. Bacteriol. **187:**3607–3616.
33. **Zweytick, D., K. Athenstaedt, and G. Daum.** 2000. Intracellular lipid particles of eukaryotic cells. Biochim. Biophys. Acta **1469:**101–120.